



저작자표시-비영리-변경금지 2.0 대한민국

이용자는 아래의 조건을 따르는 경우에 한하여 자유롭게

- 이 저작물을 복제, 배포, 전송, 전시, 공연 및 방송할 수 있습니다.

다음과 같은 조건을 따라야 합니다:



저작자표시. 귀하는 원 저작자를 표시하여야 합니다.



비영리. 귀하는 이 저작물을 영리 목적으로 이용할 수 없습니다.



변경금지. 귀하는 이 저작물을 개작, 변형 또는 가공할 수 없습니다.

- 귀하는, 이 저작물의 재이용이나 배포의 경우, 이 저작물에 적용된 이용허락조건을 명확하게 나타내어야 합니다.
- 저작권자로부터 별도의 허가를 받으면 이러한 조건들은 적용되지 않습니다.

저작권법에 따른 이용자의 권리와 책임은 위의 내용에 의하여 영향을 받지 않습니다.

이것은 [이용허락규약\(Legal Code\)](#)을 이해하기 쉽게 요약한 것입니다.

[Disclaimer](#)



TRPV5 exacerbates microglia activation-mediated neuroinflammation induced by status epilepticus

Soojin Park

**The Graduate School
Yonsei University
Department of Medical Science**

TRPV5 exacerbates microglia activation-mediated neuroinflammation induced by status epilepticus

**A Dissertation Submitted
to the Department of Medical Science
and the Graduate School of Yonsei University
in partial fulfillment of the
requirements for the degree of
Doctor of Philosophy in Medical Science**

Soojin Park

December 2024

**This certifies that the Dissertation
of Soojin Park is approved**



Thesis Supervisor Chul Hoon Kim



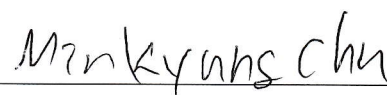
Thesis Committee Member Won-Joo Kim



Thesis Committee Member Hosung Jung



Thesis Committee Member Eunee Lee



Thesis Committee Member Min Kyung Chu

**The Graduate School
Yonsei University**

December 2024

ACKNOWLEDGEMENTS

I would like to express my deepest gratitude to those who have supported and guided me throughout the journey of completing this dissertation.

First and foremost, I am profoundly grateful to my professor, Professor Won-Joo Kim, for his unwavering support, invaluable guidance, and insightful feedback throughout this research. His expertise and encouragement were instrumental in shaping the direction of this study and fostering my growth as a researcher.

I would also like to extend my heartfelt thanks to Professor Chul Hoon Kim and my dissertation committee members, whose expertise and constructive comments significantly contributed to the quality of this work. Their rigorous evaluations and thoughtful suggestions were crucial in refining my research and enhancing the overall impact of this dissertation.

Special thanks go to Dr. Kyung Hoon Jeong for his support during the course of this research. His contributions were vital to the successful completion of this project, and his mentorship has been greatly appreciated.

I am also grateful to my colleagues and friends for their encouragement and camaraderie, which provided me with the necessary motivation and support throughout this endeavor.

Lastly, I would like to acknowledge my family for their love and understanding. Their patience and belief in me have been a constant source of strength and inspiration.

Thank you all for your invaluable contributions and support.

TABLE OF CONTENTS

LIST OF FIGURES.....	iii
LIST OF TABLES.....	iv
ABSTRACT IN ENGLISH.....	v
1. INTRODUCTION.....	1
2. MATERIALS AND METHODS.....	3
2.1. ANIMALS.....	3
2.2. PILOCARPINE-INDUCED MOUSE MODEL.....	3
2.3. LIPOPOLYSACCHARIDE (LPS)-INDUCED MICROGLIA ACTIATION <i>IN VIVO</i>	3
2.4. BRAIN TISSUE PREPARATION.....	4
2.5. IMMUNOHISTOCHEMISTRY IN BRAIN TISSUE.....	4
2.6. IMAGE ANALYSIS.....	4
2.7. MOUSE PRIMARY HIPPOCAMPAL MICROGLIA CULTURE.....	5
2.8. <i>IN VITRO</i> TREATMENTS.....	5
2.9. IMMUNOFLUORESCENCE STAINING IN CULTURED MICROGLIA.....	6
2.10. MICROGLIA MORPHOLOGY ANALYSIS.....	6
2.11. CORRECTED TOTAL CELL FLUORESCENCE (CTCF) QUANTIFICATION OF TRPV5 INTENSITY.....	6
2.12. WESTERN BLOTH ANALYSIS.....	7
2.13. <i>IN VIVO</i> DRUG ADMINISTRATION.....	8
2.14. SEIZURE MONITORING.....	8
2.15. STATISTICAL ANALYSIS.....	9
3. RESULT.....	10
3.1. CHANGE IN TRPV5 EXPRESSION IN THE HIPPOCAMPUS AFTER PILOCARPINE-INDUCED SE.....	10
3.2. TRPV5 EXPRESSION IN GLIAL CELLS IN THE HIPPOCAMPUS AFTER SE.....	12
3.3. TRPV5 EXPRESSION IN LPS-INDUCED MICROGLIA ACTIVATION <i>IN VIVO</i>	15

3.4. ACTIVATION OF PRIMARY MICROGLIA FOLLOWING LPS STIMULATION	18
3.5. INHIBITION OF TRPV5 ATTENUATED MICROGLIAL ACTIVATION.....	21
3.6. TRPV5 SUPPRESSION REDUCED ACTIVATION OF AKT/ NF-κB PATHWAY AND NLRP3 INFLAMMASOME COMPLEX DURING MICROGLIAL ACTIVATION.....	24
3.7 EFFECT OF ECONAZOLE-INDUCED TRPV5 INHIBITION IN A MOUSE MODEL OF PILOCARPINE-INDUCED SE.....	27
4. DISCUSSION.....	32
5. CONCLUSION.....	36
REFERENCES.....	37
ABSTRACT IN KOREAN.....	41

LIST OF FIGURES

<Fig. 1> Expressional changes in TRPV5 levels after SE onset.....	11
<Fig. 2> TRPV5 is predominantly expressed in activated microglia after SE induction	13
<Fig. 3> TRPV5 is expressed in activated microglia in LPS-induced neuroinflammation	16
<Fig. 4> Primary microglia activation to different doses of LPS	19
<Fig. 5> Inhibiting TRPV5 mitigates microglia activation	22
<Fig. 6> Blocking TRPV5 reduces proinflammatory cytokine production by the AKT/NF-κB Pathway and NLRP3 inflammasome in activated microglia.....	25
<Fig. 7> Effect of TRPV5 inhibition in a mouse model of pilocarpine-induced SE.....	28
<Fig. 8> Schematic representation of the role of TRPV5 in microglial activation after SE induction.....	33



LIST OF TABLES

<Table 1> Evaluation of seizure activity.....	31
---	----

ABSTRACT

TRPV5 exacerbates microglia activation-mediated neuroinflammation induced by status epilepticus

Transient receptor potential vanilloid 5 (TRPV5), a highly selective calcium ion channel, has recently been identified in various regions of the brain; however, the detailed role and underlying mechanism of TRPV5 on epileptic brain injury remains largely unexplored. In this study, I investigated the changes in TRPV5 expression in the hippocampus of a pilocarpine-induced status epilepticus (SE) mouse model and examined the effects of TRPV5 inhibition on microglial activation and neuroinflammatory responses using primary microglia culture. In the result, I confirmed that TRPV5 expression is significantly upregulated in hippocampal activated microglia after SE onset. In primary microglia culture, TRPV5 expression was upregulated in activated microglia following lipopolysaccharide (LPS) treatment, and inhibition of TRPV5 by Econazole mitigated LPS-induced microglial activation and reduced NLRP3 inflammasome formation via suppressing AKT/NF-κB signaling pathway. In the pilocarpine-induced SE mouse model, TRPV5 inhibition led to decrease in microglial activation in the hippocampus after induction of epileptic seizures. Additionally, TRPV5 inhibition markedly impaired the initiation of behavioral seizures and SE onset. Therefore, these findings demonstrate that TRPV5 is involved in microglial activation and associated neuroinflammatory responses following epileptic seizures. The present study suggests that anti-inflammatory effect by TRPV5 inhibition potentially offer new therapeutic approaches for treatment of epileptic brain damage.

Key words : epilepsy, status epilepticus, TRPV5, microglia, neuroinflammation

1. Introduction

Epilepsy is a prevalent chronic neurological disorder, characterized by spontaneous recurrent seizures¹. Temporal lobe epilepsy (TLE) is one of the most common types of focal seizures, with over 30% of patients developing resistance to conventional drug treatments². This resistance underscores the need for new and effective therapeutic strategies. Therefore, it is essential to explore novel mechanisms underlying the disease to develop more effective therapeutic approaches.

To better understand the fundamental pathophysiological mechanisms of TLE, the pilocarpine induced seizure mouse model is commonly used³⁻⁵. This well-established model closely replicates the behavioral, electrographic, and neuropathological features of human status epilepticus (SE), a critical neurological emergency characterized by continuous and self-sustaining epileptic seizures lasting more than 30 min, which can lead to severe brain injuries and an increased risk for the development of epilepsy⁶. Pilocarpine-induced SE model results in selective neuronal death, reactive gliosis, aberrant synaptic circuit organization, and abnormal neurogenesis, particularly the mossy fiber sprouting in the dentate gyrus of the hippocampus, mirroring the damage seen in human TLE⁷. In addition, inducing seizure activity in the pilocarpine model of epilepsy triggers various cellular and molecular events, such as increased neuronal excitability, perturbation of intracellular signaling pathways, and neuroinflammation⁸. These findings suggest that this model can serve as a valuable tool in epilepsy research and in developing novel therapeutic approaches. Microglia are resident immune cells of the brain that play a crucial role in maintaining brain homeostasis. As the primary defenders of the central nervous system, microglia serve as the main mediators of neuroinflammatory processes⁹. In the epileptic brain, microglia are rapidly activated¹⁰ and release proinflammatory cytokines that may cause neuronal hyperexcitability and neurodegeneration¹¹. Thus, regulating microglia activation and the resulting inflammatory response may be important in mitigating the progression of epilepsy and minimizing neurological impairments.

Transient receptor potential (TRP) channels, a family of cation channels, have become promising targets for treating various neurological disorders such as Alzheimer's disease, Parkinson's disease, Huntington's disease, and epilepsy¹². Within the TRP superfamily, the vanilloid subfamily (TRPV) consists of six members: TRPV1 to TRPV6, some of which have shown significant potential in epilepsy. For example, TRPV1 activation results in significant

microglial activation and an inflammatory reaction by inhibiting microglial transforming growth factor-beta1 signaling via interaction with Toll-like receptor 4 that indirectly enhances seizure susceptibility in hyperthermia-induced febrile seizures ¹³. Additionally, TRPV4 inhibition reduces inflammatory responses via inhibiting nucleotide-binding and oligomerization domain-like receptor family pyrin domain-containing 3 (NLRP3) inflammasome activation and neuronal cell death in mice with pilocarpine-induced SE ¹⁴. These findings suggest that TRPV channels play an important role in pathogenesis of epilepsy and epileptogenic processes.

Among the TRPV channels, TRPV5 is distinguished by its highly selective permeability to calcium ions and has been extensively studied in renal physiology ¹⁵ and osteoarthritis ^{16,17}. In osteoarthritis patient-derived chondrocytes, TRPV5 blockage reduced inflammatory cytokine expression ¹⁶, suggesting that TRPV5 is possibly involved in inflammatory response under pathological conditions. Interestingly, a recent study showed the expression of TRPV5 mRNA in the rodent brain and the predominant expression of TRPV5 in the hippocampal CA1 and CA3 regions ¹⁸; however, there is no report about how TRPV5 affects disease-related pathophysiologic features including inflammation in central nervous system disorders. Considering previous studies on the role of TRPV channels, especially TRPV1 and TRPV4, in neuroinflammation during the acute phase of epileptogenic progression, I hypothesized that TRPV5 could also be involved in the inflammatory process induced by epileptic seizures.

Therefore, in this study, I aimed to investigate whether TRPV5 could participate in epilepsy-related pathological features in the hippocampus following pilocarpine-induced SE and whether TRPV5 inhibition could regulate microglial activation and neuroinflammation.

2. Materials and Methods

2.1. Animals

All animal experiments followed the guidelines of the National Institute of Health for the Care and Use of Laboratory Animals and all animal procedures were approved by the institutional animal care and use committee (IACUC) at the Yonsei University Health System. Male C57BL/6 mice (24-25 g; Orientbio, Gyeonggi, Korea) were housed under standard temperature and humidity conditions in a 12-hour light/ dark cycle with ad libitum access to food and water.

2.2. Pilocarpine-induced mouse model

The pilocarpine-induced SE mouse model is well-established to reflect the distinct pathological characteristics of TLE, such as reactive gliosis and neuroinflammation ^{4,5,7}. For this reason, in this study, I focused on the hippocampus to investigate TRPV5 expression and its role in neuroinflammation using the pilocarpine-induced mouse model. Briefly, 30 min prior to the administration of pilocarpine (325 mg/kg, i.p.; Sigma-Aldrich, St. Louis, MO, USA), mice received an injection of scopolamine methyl nitrate (1 mg/kg, i.p.; Sigma-Aldrich) to reduce any peripheral effects. Mice reaching stages 3-5 were considered to have entered SE and were included in the experiment. SE was terminated by administration of diazepam (10 mg/kg, i.p.) 2 hours after SE induction.

2.3. Lipopolysaccharide (LPS)-induced microglia activation *in vivo*

The lipopolysaccharide (LPS)-induced microglia activation in the hippocampus was conducted as previously described ¹⁹, with some modifications. Mice were randomly divided into two groups: (1) the normal group, which received intraperitoneal vehicle (PBS) injections; and (2) the LPS group, which received intraperitoneal LPS (L2630; Sigma-Aldrich) injections at a dose of 0.5 mg/kg. Injections were daily administered for four days. Mice were euthanized and sacrificed one hour after the final injection.

2.4. Brain tissue preparation

After anesthesia with 40% urethane, the mice were euthanized via transcardial perfusion with saline, followed by 4% paraformaldehyde (PFA). The brains were then extracted, post-fixed in PFA overnight, and immersed in a 30% sucrose solution at 4°C for dehydration until fully sedimented. Following this, the brains were embedded in optimal cutting temperature (OCT) compound (Tissue-Tek, Sakura Finetek, Torrance, CA, USA) and subsequently frozen. Using a cryomicrotome (Leica Microsystems, Wetzlar, Germany), coronal brain sections were sliced to a thickness of 30 μ m and collected in 0.01M phosphate-buffered saline (PBS).

2.5. Immunohistochemistry in brain tissue

Immunohistochemistry was conducted following the method previously established ²⁰, with slight modifications. After blocking in 5% normal horse serum (Vector Laboratories, Burlingame, CA, USA) in 0.01M PBS for 1 hour at room temperature, tissue sections were incubated overnight at 4°C with the following primary antibodies: rabbit anti-transient receptor potential vanilloid 5 (TRPV5; ab137028; Abcam, Cambridge, MA, USA), mouse anti-glial fibrillary acidic protein (GFAP; MAB360; Millipore), goat anti-ionized calcium-binding adapter molecule-1 (Iba1; ab5076; Abcam). The following day, the sections were incubated with fluorescence-conjugated secondary antibodies for 2 hours. The stained sections were cover slipped using hardset antifade mounting medium with DAPI (Vectashield; CA, USA) and observed under a fluorescence microscope (Axio Imager M2; Carl Zeiss, Thornwood, NY, USA). Images were captured using a confocal laser scanning microscope (LSM 700; Carl Zeiss). The immunoreactivity of TRPV5-positive cells and Iba1-expressing microglia were analyzed in the subpyramidal area of the hippocampus between bregma – 1.46 and – 2.30 mm, as previously described ²⁰. The quantitative analyses were performed using Fiji software (ImageJ; National Institutes of Health, Bethesda, MD, USA).

2.6. Image analysis

Pearson Correlation Coefficient (PCC) analysis is a statistical method commonly used to assess the degree of colocalization between two fluorescent signals, which can provide the specific cellular phenotype of the target protein. In our study, PCC analysis was employed using ImageJ

software to evaluate the degree of colocalization between TRPV5 and glial cells (GFAP: astrocyte marker; Iba1: microglia cell marker) in the subpyramidal area of the hippocampus following SE induction. Colocalization was measured by calculating the correlation coefficients to evaluate the overlap of fluorescent signals. The correlation coefficients were interpreted as follows: 0 – 0.19 indicating 'very weak' correlation, 0.20 – 0.39 indicating 'weak' correlation, 0.40 – 0.59 indicating 'moderate' correlation, 0.60 – 0.79 indicating 'strong' correlation, and 0.80 – 1.0 indicating 'very strong' correlation²¹.

2.7. Mouse primary hippocampal microglia culture

Primary hippocampal microglia were harvested and cultured as previously described with some modifications²². Briefly, adult C57BL/6J mice (8 weeks old; Orientbio) were euthanized via cervical dislocation and decapitated. The brains were removed and placed in ice cold dissection media (Minimal essential media (MEM; Gibco, CA, USA) with 1% penicillin-streptomycin (PS; Gibco), 2.5% HEPES buffer solution (Gibco) and 1% 1M Tris solution). The hippocampi were then isolated, dissociated, and cultured in complete media (Dulbecco's Modified Eagle Medium F12 (DMEM/F12; Gibco) supplemented with 10% fetal bovine serum (FBS; Moregate, Australia), 1% PS and 1% GlutaMAX (Gibco)) for 6 hours. Microglia were isolated by repeated tapping to remove non-adherent cells, resulting in a pure culture of adherent, adult mouse microglia. Subsequently, the isolated microglia were randomly allocated to different treatment groups and incubated in T₂₅ flasks at 37°C in a humidified 5% CO₂ atmosphere for 4 days. Cells were then harvested and plated onto culture plates or cover glasses for each experiment. After 3 days, half of the complete media were replaced with fresh media and cells were incubated for 1 hour.

2.8. *In vitro* treatments

To evaluate the activation of microglia in response to LPS stimulation, microglial cells were divided into three groups: (1) a control group with no exposure to LPS, (2) a group exposed to 1 ng/ml of LPS, and (3) a group exposed to 10 ng/ml of LPS for 24 hours. To evaluate the effect of TRPV5 inhibition in LPS stimulated mice, microglial cells were pre-treated with Econazole (Eco; S5492; Selleck Chemicals, Munich, Germany), a potential TRPV5 inhibitor²³. Cells were divided into three groups: (1) a group with no Eco treatment, (2) a group treated with 0.1 µmol/L of Eco, and (3) a group treated with 1.0 µmol/L of Eco. After 24 hours of pre-treatment with Eco, all

groups were then exposed to 10 ng/ml of LPS for an additional 24 hours.

2.9. Immunofluorescence staining in cultured microglia

In brief, primary cultured cells were washed with Dulbecco's phosphate-buffered saline (dPBS; Gibco) and fixed with 4% PFA/ 4% sucrose for 15 min in room temperature and then washed with dPBS. The cells were then permeabilized with 0.01% Triton X-100 in dPBS for 15 min. After blocking in 5% bovine serum albumin (Bovogen Biologicals, MEL, Australia) in dPBS for 1 hour, the cells were incubated overnight at 4°C in dPBS containing primary antibodies: rabbit anti-TRPV5 (Abcam) and goat anti-Iba1 (Abcam). This was followed by incubation with appropriate fluorescence-conjugated secondary antibodies for 2 hours at room temperature. After washing, the cells were counter-stained with HOESCHST 33258 (Molecular Probes, Eugene, OR, USA) for 20 min at room temperature. The cells were mounted on slides and examined using a fluorescence microscope (Axio Imager M2). Confocal laser scanning microscopy (LSM 700) was used to capture the images.

2.10. Microglia morphology analysis

As previously described²⁴, microglia with long, thin processes and small cell soma were classified as being in the resting form, while cells with short, sturdy processes and enlarged cell soma were classified as being in the activated form. The number of cells was manually counted according to their morphology, and the percentages of resting and activated forms were calculated among the total microglia cells under different conditions. At least 5 randomly selected fields were used for quantification.

2.11. Corrected Total Cell Fluorescence (CTCF) quantification of TRPV5 intensity

Corrected Total Cell Fluorescence (CTCF) is a widely recognized method used to quantify fluorescence intensity, accounting for background signal, and providing a more accurate measurement of the true fluorescence emitted by the cells²⁵. CTCF was employed to quantify TRPV5 fluorescence intensity in microglial cells exposed to varying concentrations of Econazole (0.1 and 1 μ mol/L) along with LPS stimulation using ImageJ software. CTCF values were

calculated by manually outlining microglial cells and extracting key parameters, such as the total area of each microglial cell, the mean fluorescence intensity, and the integrated density (total fluorescence). Adjacent background regions were also selected to obtain reliable background measurements for accurate subtraction from the microglial signal. These extracted values were then measured in the corrected total cell fluorescence equation, which computes individual CTCF metrics: $CTCF = \text{Integrated density} - (\text{area of selected cell} * \text{mean fluorescence of background readings})$. This method ensured that the calculated fluorescence intensity reflected the actual expression levels of TRPV5, minimizing the influence of non-specific background fluorescence.

2.12. Western blot analysis

Western blot samples were prepared as described previously²⁶. Briefly, isolated hippocampi tissue or cultured primary microglia were resuspended in sodium dodecyl sulfate (SDS) lysis buffer or radioimmunoprecipitation assay (RIPA) lysis buffer, respectively, and centrifuged at 4°C for 15 min at 14,000g. The protein concentration of the supernatants was quantified using a bicinchoninic acid assay kit (Thermo Scientific, Rockford, IL, USA). Proteins were separated using SDS-polyacrylamide gel electrophoresis with appropriate molecular weight markers (Thermo Scientific) and transferred onto polyvinylidene difluoride membranes (Millipore) using an electrophoretic transfer system (Bio-Rad Laboratories, Hercules, CA, USA.). After blocking in 5% skim milk in 1X tris-buffered saline with 0.1% Tween 20 (TBST) for 1 hour, the membranes were incubated overnight at 4°C with specific primary antibodies: rabbit anti-TRPV5 (1:1000; Abcam), goat anti-Iba1 (1:1000; Abcam), rabbit anti-phospho-nuclear factor-κB (p-NF-κB; #3033; 1:1000; Cell Signaling Technology), mouse anti-NF-κB (#6956; 1:1000; Cell Signaling Technology), mouse anti- NLRP3 (AG-20B-0014; 1:1000; AdipoGen, San Diego, CA, USA), mouse anti-apoptosis-associated speck-like protein containing a caspase-recruitment domain (ASC; AG-25B-0006; 1:1000; AdipoGen), rabbit anti-Caspase 1 (AG-20B-0042; 1:1000; AdipoGen), anti p-protein kinase B (Ser473) (p-AKT; #9271; 1:1000; Cell signaling technology), anti-AKT (#9272; 1:1000; Cell signaling technology), anti-Interleukin-18 (IL-18; #PA5-79481; 1:1000, Invitrogen, Waltham, MA, USA) and mouse anti-β-actin (sc-47778; 1:4000; Santa Cruz Biotechnology, Dallas, TX, USA). After washing, membranes were incubated with secondary antibodies (1:10000; Enzo Life Science, Farmingdale, NY, USA), and the blots were developed using ECL western blotting detection reagents (Amersham Biosciences, Piscataway, NJ, USA).

Protein bands were measured using a computer imaging device and accompanying software (Fujifilm; Tokyo, Japan).

2.13. *In vivo* drug administration

Econazole was first dissolved in 100% ethanol and then diluted in a vehicle solution containing 5% Tween 80, 5% polyethylene glycol 400 (Sigma-Aldrich), and 4% ethanol, prepared immediately before injection. To assess the effects of TRPV5 inhibition on seizure activity and microglia activation, mice were divided into two groups: (1) vehicle treated SE group (SE_Veh; mice treated with the vehicle and subjected to SE) and (2) Eco treated SE group (SE_Eco; mice treated with Eco and subjected to SE). Initially, mice were pretreated with Eco at a dose of 40 mg/kg (i.p.) or with the vehicle for three consecutive days prior to pilocarpine induction. One hour after seizure termination with diazepam, the mice received their fourth injection of Eco or vehicle, followed by daily injections for three additional days. The mice were sacrificed four days after SE induction for further analysis.

2.14. Seizure monitoring

Mice were continuously monitored and seizure behavioral stages were assessed using the Racine scale²⁷, which includes: stage 1, facial movement; stage 2, head nodding; stage 3, forelimb clonus; stage 4, rearing; and stage 5, rearing and falling. Seizures were defined as behaviors corresponding to Racine stages 3-5, and the number of such seizures was counted before mice reached SE. Mice reaching these stages followed by continuous motor activity for more than 10 minutes were considered to have entered SE and included in the experiment. To assess the onset time of convulsive seizures and latency to SE onset, mice were continuously monitored from the time of pilocarpine administration until the termination of seizures, as previously described²⁸. The percentage of animals reaching SE onset was calculated based on the total number of animals. Mortality was expressed as the percentage of surviving and deceased animals relative to the total number. The maximal seizure score for each animal, defined as the highest seizure stage reached prior to SE onset, was recorded, and the average maximal score across both groups was calculated. Additionally, the number of seizures each animal experienced before entering SE was recorded. The onset time of convulsive seizure was defined as the elapsed time from pilocarpine injection to the first seizure with a Racine score of stage 3 or higher. The latency to SE onset was determined

as the time from pilocarpine injection to the onset of SE.

2.15. Statistical analysis

Statistical analyses were conducted using GraphPad Prism 9 (GraphPad Software, Inc., San Diego, CA, USA). Data are expressed as means \pm standard error of the mean (SEM), with individual data points displayed. One-way analysis of variance (ANOVA) followed by Tukey's multiple comparison test was applied for comparisons between groups. A threshold of $p < 0.05$ was set for statistical significance. Detailed p -values and sample sizes for each experiment are included in the respective figure legends.

3. Result

3.1. Change in TRPV5 expression in the hippocampus after pilocarpine-induced SE

To investigate the changes in TRPV5 expression after SE induction, I first examined its distribution and expression in the mouse hippocampus following SE injury. TRPV5 immunoreactivity was significantly elevated 4 days after SE induction compared to sham mice, with a slight decrease observed by day 7 (Fig. 1A). Interestingly, 4 days post-SE, TRPV5 expression was primarily observed in non-neuronal, glial-like cells. Consistent with the immunostaining results, the protein levels of TRPV5 showed significant up-regulation in the hippocampus at both 4 days ($p = 0.003$ vs. sham) and 7 days ($p = 0.022$ vs. sham) post-SE (Fig. 1B and C) compared to sham-manipulated mice.

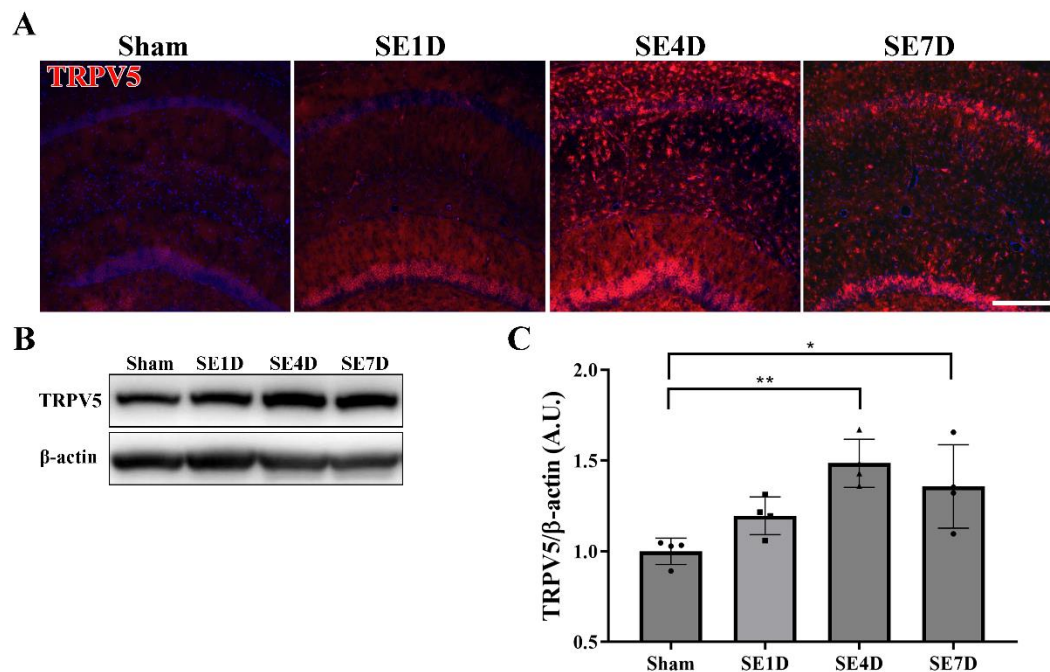


FIGURE 1. Expressional changes in TRPV5 levels after SE onset. A) Representative TRPV5 immunohistochemistry of hippocampal CA1 regions in sham and SE-induced mice at various time points in vivo. Scale bar = 200 μ m. **B)** Representative immunoblots of TRPV5 expression at different time points after SE induction. **C)** TRPV5 protein bands were quantified and normalized against the expression of the housekeeping protein β -actin. ** p < 0.01 versus Sham; * p < 0.05 versus Sham (one-way ANOVA followed by Tukey's post hoc test). Values are expressed as a mean \pm SEM.

3.2. TRPV5 expression in glial cells in the hippocampus after SE

To identify changes in glial TRPV5 expression in the hippocampus 4 days after SE induction, TRPV5 was co-stained with either the astrocyte marker GFAP or the microglia marker Iba1. The colocalization analysis between TRPV5 and GFAP revealed a weak correlation ($r = -0.01822$, Fig. 2A). Subsequent double-staining with TRPV5 and Iba1 showed predominant TRPV5 expression in microglia, with a high degree of colocalization between TRPV5 and Iba1 signals ($r = 0.77287$, Fig. 2B). These findings indicate significant localization of TRPV5 expression within activated microglia following SE induction.

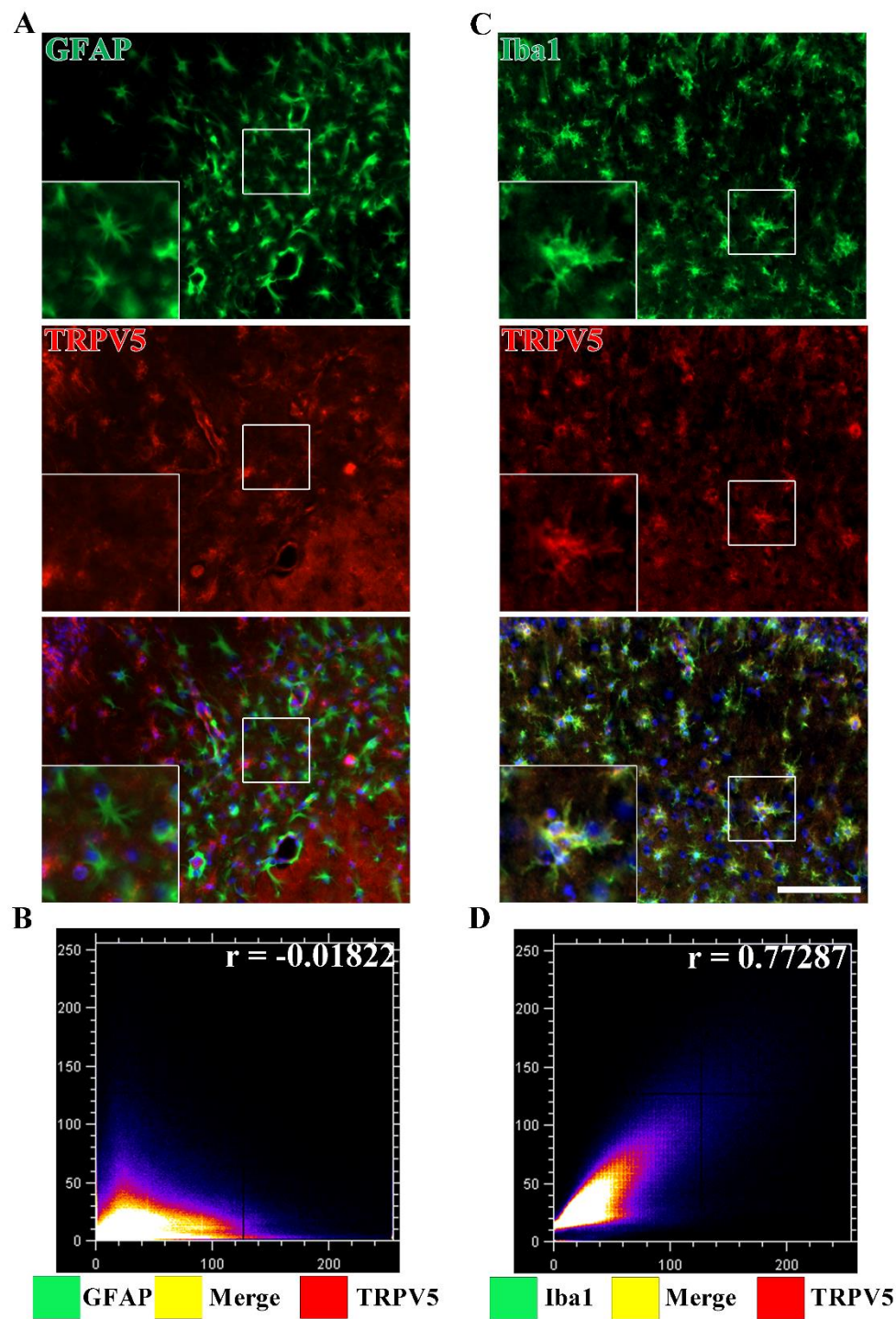


FIGURE 2. TRPV5 is predominantly expressed in activated microglia after SE induction. A) Representative double immunohistological images of GFAP-positive astrocytes (green) and TRPV5 (red) in the hippocampus 4 days post-SE. Scale bar = 100 μ m. **B)** Graphic representation (scatter plot) of the Pearson correlation of coefficient (PCC) for quantifying the colocalization between TRPV5 and GFAP in hippocampus after SE. **C)** Representative double immunohistological staining for Iba1-expressing microglia (green) and TRPV5 (red) in the hippocampus 4 days post-SE. **D)** Graphic representation (scatter plot) of the PCC for quantifying the colocalization between TRPV5 and Iba1 in hippocampus after SE.

3.3. TRPV5 expression in LPS-induced microglia activation *in vivo*

LPS is a well-established agent used to induce the microglial activation and a robust inflammatory response^{29,30}. Given our results showing upregulation of TRPV5 in activated microglia following epileptic seizures (Fig. 2), I further identified the cellular phenotype of TRPV5 expression in activated microglia following LPS treatment. To address the identification of TRPV5 upregulation within activated microglia, I examined the expressional pattern of TRPV5 in glia cells in the mouse hippocampus after receiving daily LPS injections at a dose of 0.5 mg/kg for four consecutive days (Fig. 3). Double-immunostaining was carried out, and Pearson correlation coefficient analysis revealed that TRPV5 expression was predominantly expressed in Iba1-positive microglia cells ($r = 0.64575$), similar to the findings at 4 days post-SE.

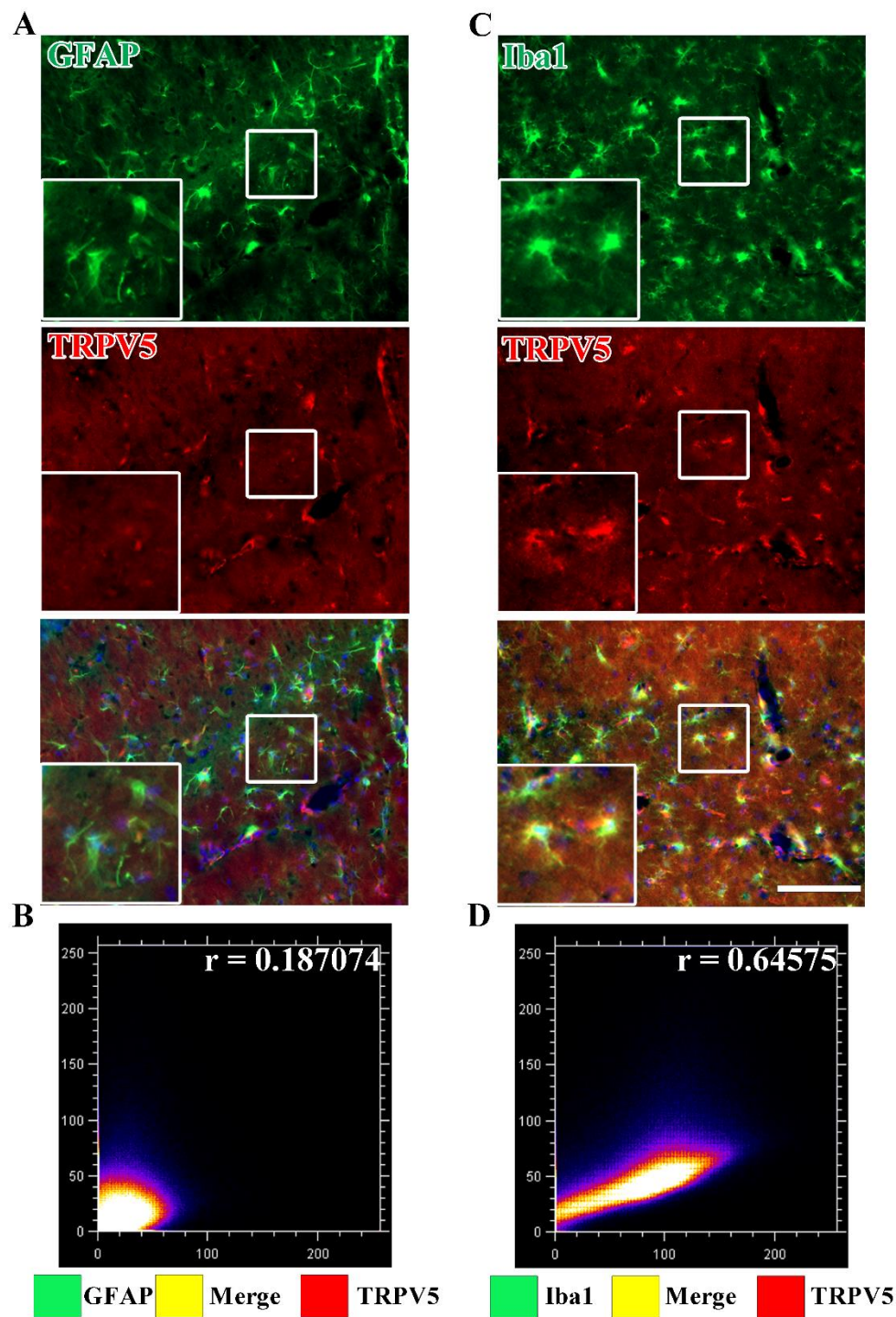


FIGURE 3. TRPV5 is expressed in activated microglia in LPS-induced neuroinflammation.

A) Representative double immunohistochemical images of GFAP-positive astrocytes(green) and TRPV5 (red) in the hippocampus after four consecutive days of daily LPS injections. Scale bar =100 μ m. **B)** Scatter plot showing the PCC quantifying the colocalization between TRPV5 and GFAP in hippocampus after LPS injections. **C)** Representative double immunohistochemical images for Iba1-expressing microglia (green) and TRPV5 (red) in the hippocampus after four daily injections of LPS. **D)** Scatter plot showing the Pearson correlation coefficient quantifying the colocalization between TRPV5 and Iba1 in hippocampus after LPS injections.

3.4. Activation of primary microglia following LPS stimulation

The use of a cell model is suitable for exploring the functional role and related cellular/molecular mechanism of activated microglia under epileptic conditions. Although there is no suitable cell model that can fully replicate the inflammatory process associated with epilepsy, LPS-stimulated microglia are a well-established *in vitro* model for studying inflammatory responses. For example, LPS stimulates the activation of cultured microglia cells and activates the AKT/NF-κB signaling pathway, leading to the formation of the NLRP3 inflammasome³¹. These phenomena are similarly detected in the damaged hippocampus following the pilocarpine-induced SE *in vivo*³². Therefore, these suggest that the LPS-stimulated microglia *in vitro* model can be utilized to investigate the mechanisms involved in neuroinflammation induced by epileptic seizures^{29,33}.

In this study, to examine the influence of TRPV5 on microglial activation and related inflammatory responses, primary hippocampal microglia were exposed to the different-doses of LPS (10 or 100 ng/ml) for 24 hours (Fig. 4). For morphological analysis, Iba1-expressing primary microglial cells were distinguished based on their shapes as follows: amoeboid-like cells without thin processes were referred to as activated microglia (indicated by filled arrows in Fig. 4A), while flat cells with multiple thin processes were defined as resting microglia (indicated by empty arrows in Fig. 4A). Microglia treated with vehicle solution exhibited a polarized morphology with thin processes, showing the microglia in resting state (Fig. 4A). In contrast, microglia treated with 10 ng/ml LPS exhibited morphological changes, including shortened processes and slightly enlarged cell bodies, indicating activation (Fig. 4A). Microglia exposed to 100 ng/ml LPS displayed more pronounced morphological changes, such as amoeboid-like cells without thin processes, adopting a typical morphology of activated microglia (Fig. 4A). In line with these morphological changes, quantitative analysis revealed a significant increase in the percentage of activated microglia ($p < 0.001$ vs. Veh, Fig. 4B), suggesting that LPS stimulation could successfully trigger the microglial activation. Based on these results, the LPS dose was standardized at 100 ng/ml for subsequent experiments.

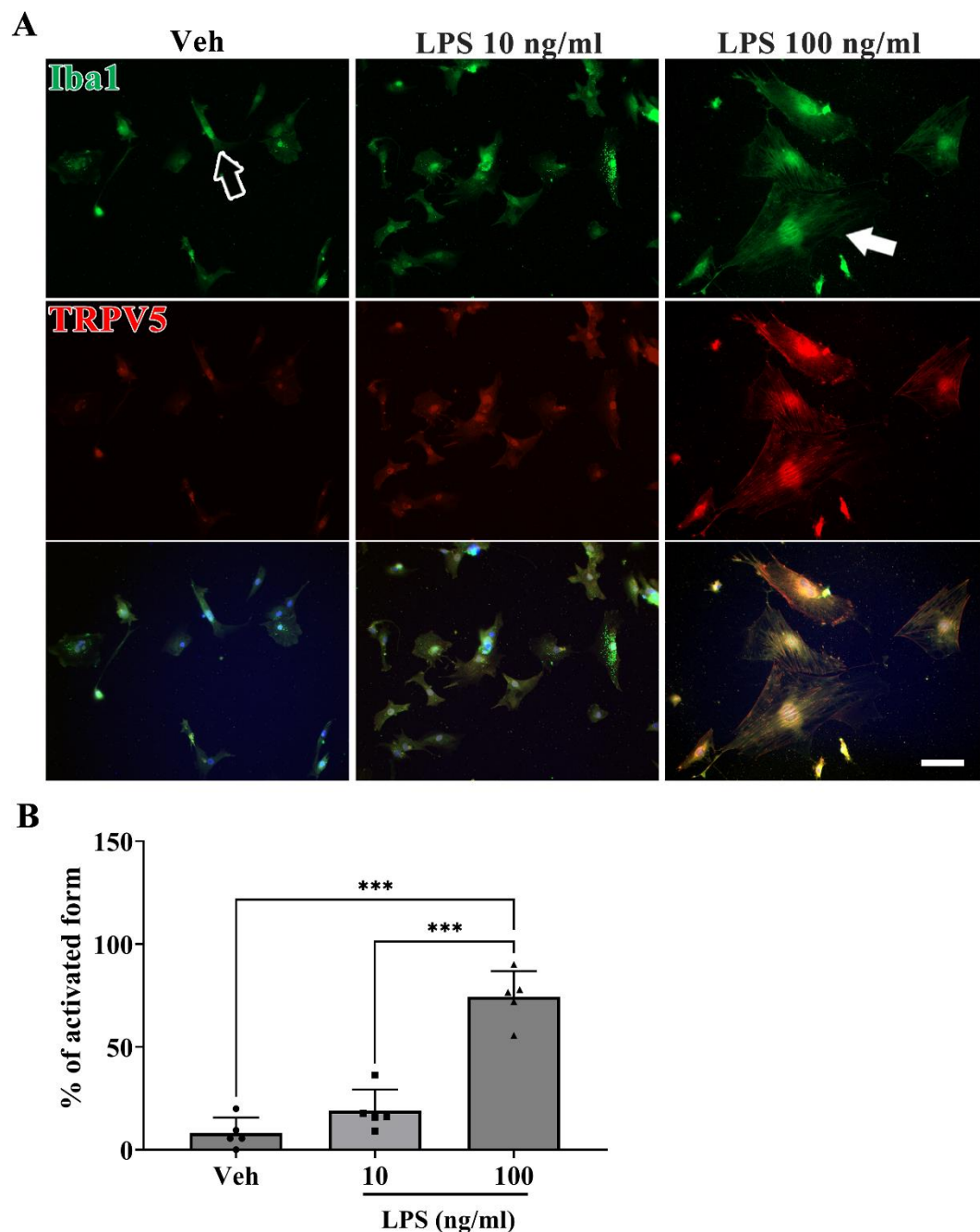


FIGURE 4. Primary microglia activation to different doses of LPS. A) Immunocytochemistry images depict TRPV5-Iba1 double-positive cells in primary cultured microglia treated with

varying concentrations of LPS (10 or 100 ng/ml) for 24 hours. Empty arrow indicates microglia in their resting form and filled arrow shows microglia in activated form. Scale bar = 20 μ m **B**)
Graphic representations illustrate the percentage of microglia in activated state under each condition. The percentage of activated microglia significantly increased post-LPS treatment. *** p < 0.001, Veh vs. LPS_10; *** p < 0.001, Veh vs. LPS_100 (ANOVA followed by Tukey's post hoc test).

3.5. Inhibition of TRPV5 attenuated microglial activation

To confirm the efficacy of pharmacological inhibition of TRPV5 with Econazole, a potential inhibitor of TRPV5, I initially assessed the expressional change of TRPV5 across various experimental conditions: normal cells, normal cells treated with 0.1 or 1.0 μ mol/L Econazole (Fig. 5A), cells stimulated with LPS, and cells pretreated with 0.1 or 1.0 μ mol/L Econazole followed by LPS stimulation (Fig. 5B). The fluorescence intensity of TRPV5, upregulated by LPS stimulation ($p < 0.001$ vs. LPS), was significantly reduced in cultured microglia treated with both 0.1 and 1.0 μ mol/L Econazole ($p = 0.042$, LPS vs. LPS_Eco 0.1, $p < 0.001$, LPS vs. LPS_Eco 1.0; Fig. 5C), indicating that Econazole acts as a TRPV5 inhibitor.

Next, I investigated the effect of TRPV5 inhibition by treatment with 0.1 and 1.0 μ mol/L Econazole in LPS-activated microglia, as analyzing the morphological changes in primary microglia (Fig. 5C). The percentage of activated microglia, characterized by an amoeboid-like morphology, that was significantly increased by LPS stimulation ($p < 0.001$, Nor vs. LPS) was drastically decreased with TRPV5 inhibition in both doses of Econazole ($p < 0.001$, LPS vs. LPS_Eco 0.1; $p < 0.001$, LPS vs. LPS_Eco 1.0; Fig. 5C). The higher dose of Econazole resulted in a greater decrease in the fluorescence intensity of TRPV5, thereby the Econazole dose was standardized at 1.0 μ mol/L in the following experiments. Taken together, these findings suggest that TRPV5 inhibition dramatically reduces microglial activation.

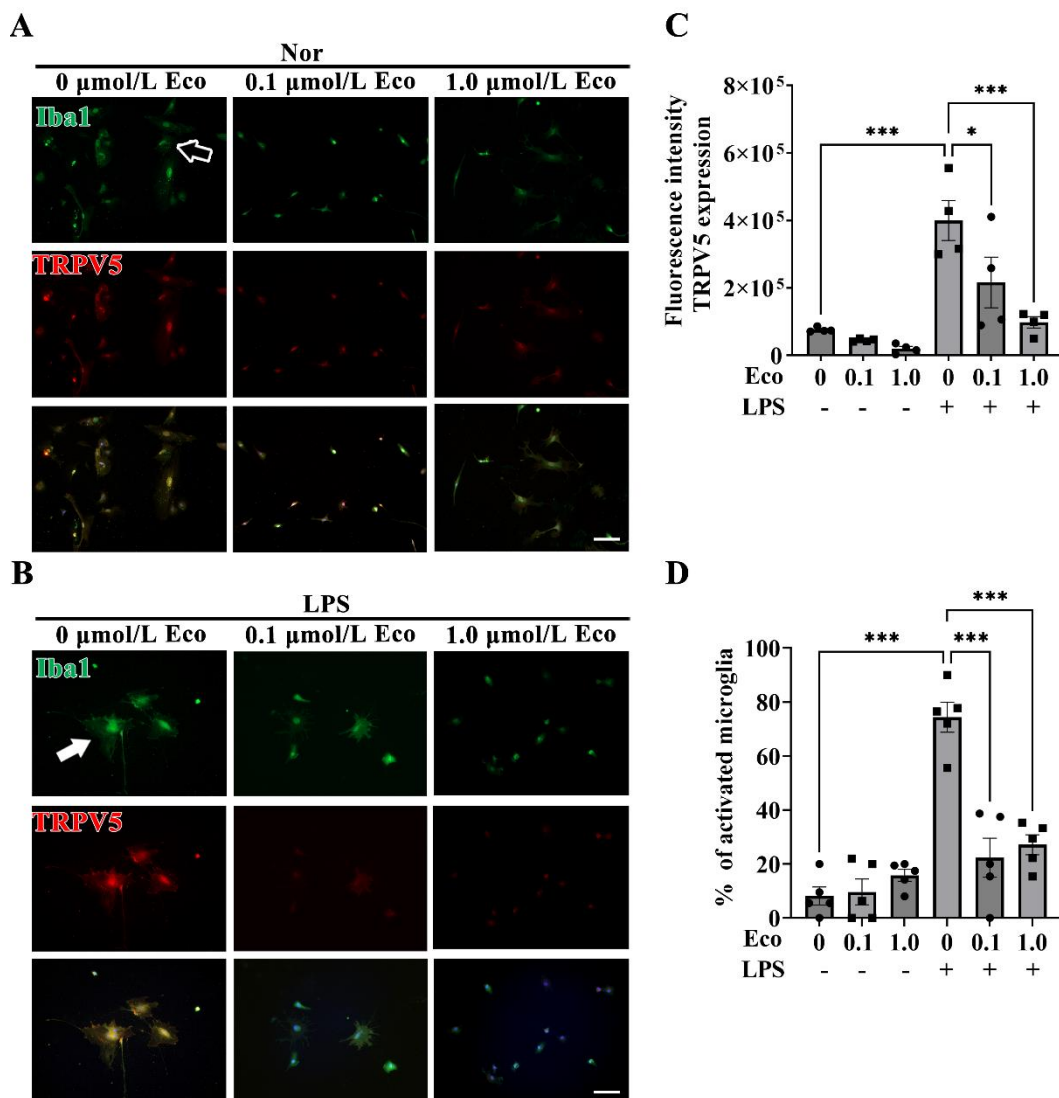


FIGURE 5. Inhibiting TRPV5 mitigates microglia activation. **A)** Immunocytochemistry images depict TRPV5-Iba1 double-positive cells in primary cultured microglia, treated with different doses of the TRPV5 inhibitor, Econazole (0.1 or 1.0 $\mu\text{mol/L}$), for 24 hours in normal cells. Empty arrow indicates microglia in resting form. Scale bar = 20 μm **B)** Immunocytochemistry images showing TRPV5-Iba1 double-positive cells in primary cultured microglia, treated with different doses of Econazole, for 24 hours prior to LPS stimulation. Filled arrow shows microglia in activated form. Scale bar = 20 μm **C)** Bar plot of TRPV5 fluorescence intensity under various

conditions. **D)** Graph representing the percentage of activated microglia under various conditions.
*** $p < 0.001$, Nor vs. LPS; *** $p < 0.001$, LPS vs. LPS_Eco 0.1; *** $p < 0.001$, LPS vs LPS_Eco 1.0 (ANOVA followed by Tukey's post hoc test).

3.6. TRPV5 suppression reduced activation of AKT/ NF-κB pathway and NLRP3 inflammasome complex during microglial activation

Based on our results (Fig. 5), I investigated whether TRPV5 inhibition could be involved in microglial-derived inflammatory processes using western blotting (Fig. 6A and 6D). Our results showed a significant suppression in the protein levels of phosphorylated AKT ($p = 0.0026$, LPS_Veh vs. LPS_Eco, Fig. 6B), phosphorylated NF-κB ($p = 0.002$, LPS_Veh vs. LPS_Eco, Fig. 6C), and the NLRP3 inflammasome complex (NLRP3: $p = 0.0013$, LPS_Veh vs. LPS_Eco, Fig. 6E; Caspase1: $p = 0.0433$, LPS_Veh vs. LPS_Eco, Fig. 6F; ASC: $p = 0.0046$, LPS_Veh vs. LPS_Eco, Fig. 6G) in activated microglia under conditions where TRPV5 was inhibited. Moreover, Econazole treatment significantly reduced the protein level of IL-18, a proinflammatory cytokine, compared to that of the LPS-treated group ($p = 0.0046$, LPS_Veh vs. LPS_Eco, Fig. 6H). These results suggest that blocking TRPV5 can reduce AKT/NF-κB activation and NLRP3 inflammasome-mediated proinflammatory cytokine release in microglia following LPS stimulation.

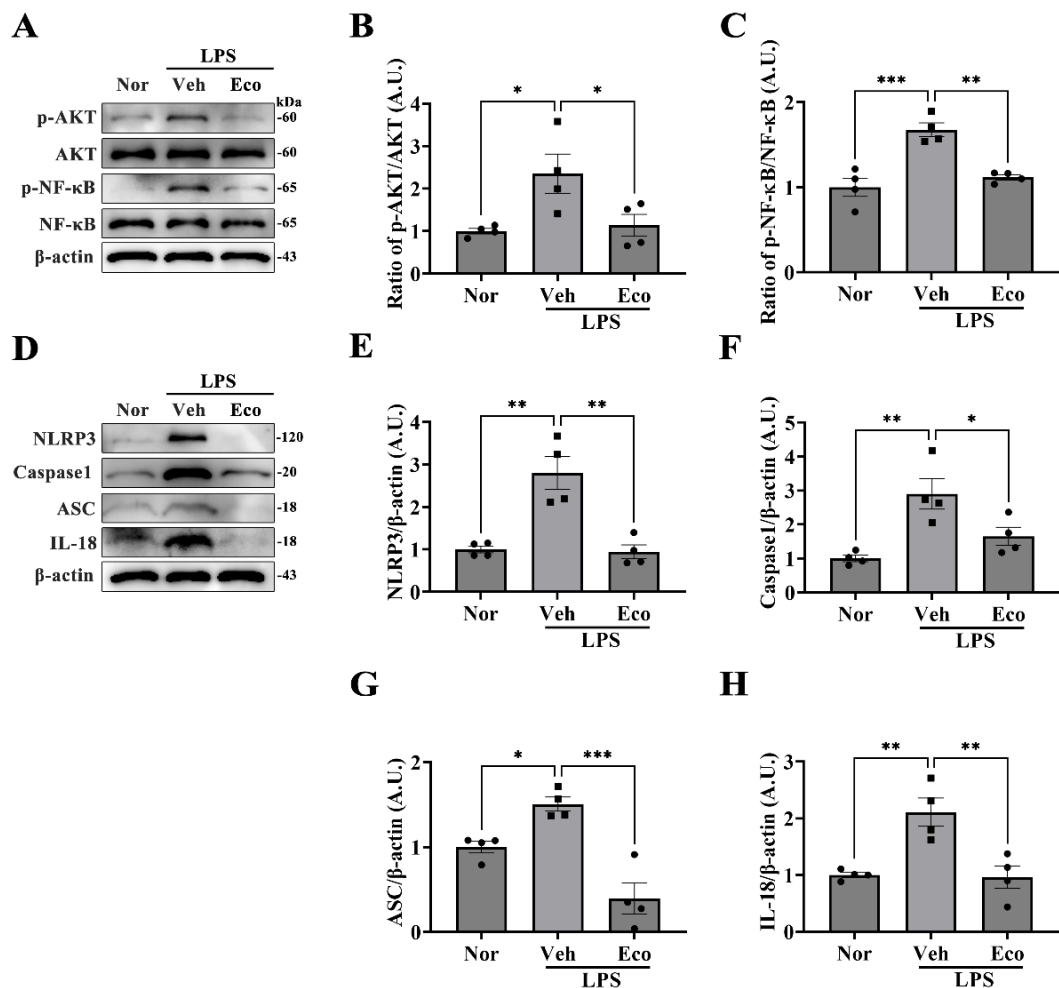


FIGURE 6. Blocking TPRV5 reduces proinflammatory cytokine production by the AKT/NF-κB pathway and NLRP3 inflammasome in activated microglia. **A)** Representative blots showing p-AKT, AKT, p-NF-κB, NF-κB, and β-actin expression in each group. **B)** Histogram showing the ratio of p-AKT to AKT protein bands quantified and normalized against the expression of the housekeeping protein β-actin. $*p < 0.05$, significantly different from each group (ANOVA followed by Tukey's post hoc test, $n = 4$ per group). **C)** Histogram showing the ratio of p-NF-κB to NF-κB protein bands quantified and normalized against the expression of the β-actin. $***p < 0.001$ and $**p < 0.01$, significantly different from each group (ANOVA followed by Tukey's post hoc test). **D)**

Representative blots showing NLRP3, Caspase 1, ASC, IL-18, and β -actin expression in each group.

E) Histogram showing NLRP3 expression. ** p < 0.01, significantly different from each group (ANOVA followed by Tukey's post hoc test). **F)** Histogram showing Caspase 1 expression. ** p < 0.01 and * p < 0.05, significantly different from each group (ANOVA followed by Tukey's post hoc test). **G)** Histogram showing ASC expression. *** p < 0.001 and * p < 0.05, significantly different from each group. (ANOVA followed by Tukey's post hoc test). **H)** Histogram showing IL-18 expression. ** p < 0.01, significantly different from each group (ANOVA followed by Tukey's post hoc test). All values are presented as mean \pm SEM with individual data points indicated.

3.7. Effect of Econazole-induced TRPV5 inhibition in a mouse model of pilocarpine-induced SE

Based on our above results, I further examined whether TRPV5 inhibition by Econazole treatment could affect hippocampal microglia activation in a mouse model of pilocarpine-induced SE. To evaluate the effect of TRPV5 inhibition on microglial activation induced by pilocarpine-induced SE, Econazole (40 mg/kg, i.p.) was pre-treated for 3 days before pilocarpine-induced SE and given daily for 4 days starting at 1 hour after seizure termination. I observed that TRPV5 immunoreactivity was upregulated four days after SE induction ($p < 0.001$ vs. SE4D_Veh). However, this upregulation was significantly reduced by Econazole treatment ($p < 0.001$ vs. SE4D_Eco; Fig. 7A), suggesting that Econazole effectively functions as a TRPV5 inhibitor in vivo (Fig. 7B). Additionally, the expression of Iba1-positive microglia was increased in the hippocampus of Veh-SE4D group ($p < 0.001$ vs. SE4D_Veh), but treatment with Econazole significantly reduced pilocarpine-induced microglial activation ($p < 0.001$ vs. SE4D_Eco; Fig. 7C). In addition to *in vitro* result in this study, these findings indicate that TRPV5 is involved in microglial activation following epileptic seizures.

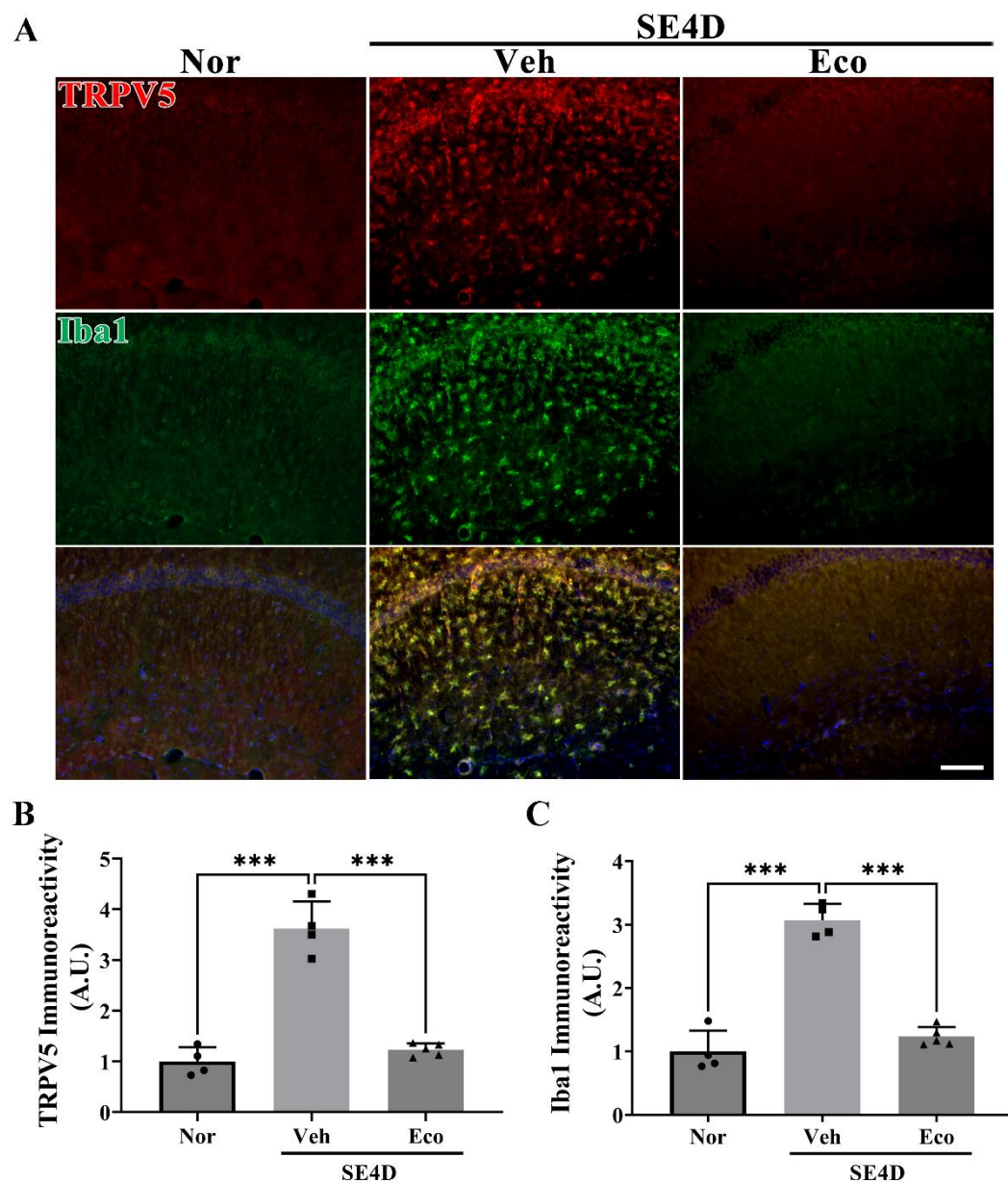


FIGURE 7. Effect of TRPV5 inhibition in a mouse model of pilocarpine-induced SE. A) Representative double immunohistochemistry images showing upregulated TRPV5 (red) and activated microglia (green) 4 days post-SE, with a decrease observed in the TRPV5-inhibited group. Scale bar = 100 μ m. **B)** Quantitative analysis of TRPV5 immunoreactivity expressed as



mean \pm SEM with individual data points indicated. *** $p < 0.001$, significantly different from each group (ANOVA followed by Tukey's post hoc test). **C**) Quantitative analysis of Iba1 immunoreactivity presented as mean \pm SEM with individual data points indicated. *** $p < 0.001$, significantly different from each group (ANOVA followed by Tukey's post hoc test)

Furthermore, I evaluated the effect of TRPV5 inhibition via treatment with Econazole on pilocarpine-induced seizure activity. Seizure parameters were analyzed across both the treated and control groups (Table 1). Although there were no significant differences between the groups in terms of the percentage of animals reaching SE onset, mortality rates, maximal seizure scores, and the number of seizures prior to SE onset, Econazole treatment significantly delayed the onset of both convulsive seizures and SE (onset time of convulsive seizures: $p < 0.001$ vs. SE-Veh; latency to SE onset: $p < 0.001$ vs. SE-Veh). These results suggest that TRPV5 inhibition could exert anti-convulsive effects against the initiation and development of epileptic seizures.

TABLE 1. Evaluation of seizure activity

	SE_Veh (n = 10)	SE_Eco (n = 10)	p value
Animals reaching SE onset (%)	100	100	> 0.999
Mortality (%)	30	30	> 0.999
Maximal seizure score	4.2 ± 0.200	3.7 ± 0.133	0.113
No. of seizures before entering SE	2.9 ± 0.180	3 ± 0	0.584
Onset time of convulsive seizure (min)	16 ± 2.216	28.2 ± 1.775	< 0.001
SE onset time (min)	33 ± 2.673	55.8 ± 2.602	< 0.001

4. Discussion

TRPV channels, including TRPV1 and TRPV4, have been implicated in various epileptogenic processes, demonstrating their role in the pathological mechanisms in epilepsy. Despite this, the involvement of TRPV5 in neuropathological conditions, particularly epilepsy, remains unexplored. The present study provides the first evidence of TRPV5 upregulation in the hippocampus after SE induction, predominantly in hippocampal microglia. Inhibition of TRPV5 with Econazole in cultured primary microglia led to significant suppression of LPS-stimulated microglial activation and blockade of inflammatory process, characterized by decreased AKT/NF-κB signaling and reduced NLRP3 inflammasome-mediated proinflammatory cytokine production. Additionally, TRPV5 inhibition suppressed microglial activation in a mouse model of pilocarpine-induced SE. TRPV5 suppression mitigated the initiation of behavioral seizures and delayed the onset of SE induction. Taken together, these findings suggest that TRPV5 plays a crucial role in microglia activation and associated neuroinflammation under neuropathological condition following epileptic seizures (Figure 8).

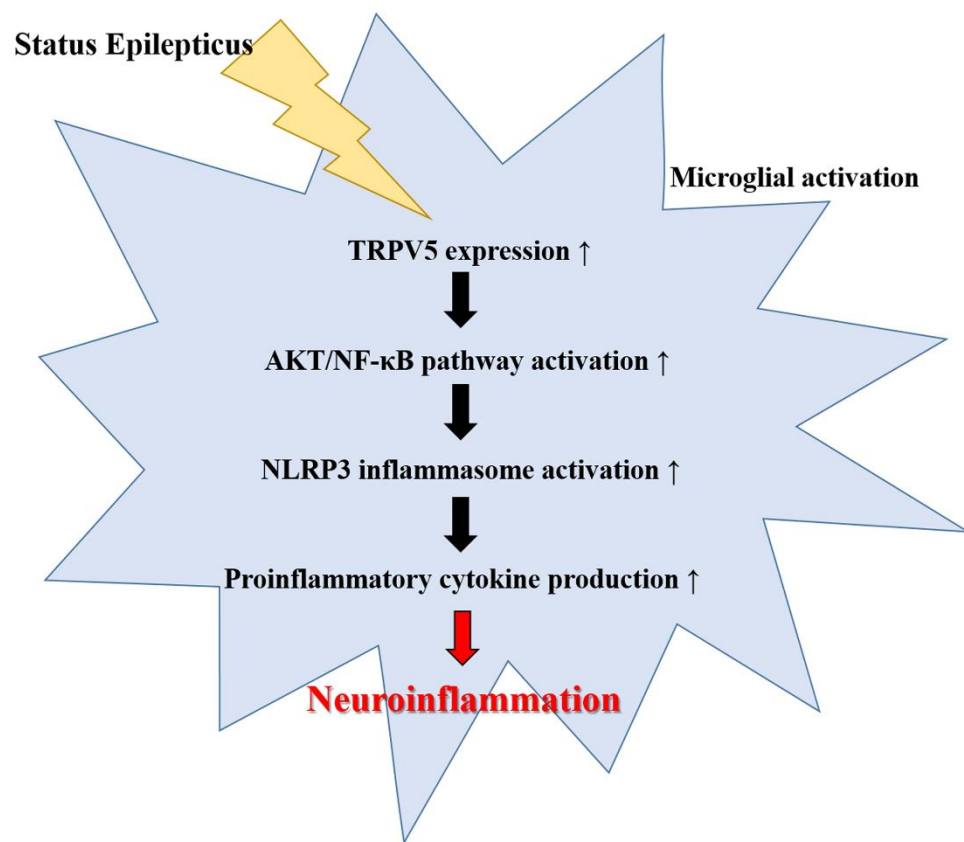


FIGURE 8. Schematic representation of the role of TRPV5 in microglial activation after SE induction.

Microglia, the resident immune cells of the brain, play crucial roles in immune surveillance and maintaining brain homeostasis³⁴. In epilepsy, activated microglia release various proinflammatory cytokines that can lower seizure threshold and enhance neuronal excitability^{11,35}. This cytokine-driven inflammatory state contributes to sustained neuronal damage and epileptogenesis. In line with this evidence, minocycline, a microglial activation inhibitor^{36,37}, significantly reduces neuronal damage in kainic acid-induced SE models³⁸ and decreases seizure duration and severity and lower SE-induced cytokine levels in pilocarpine-induced SE models³⁹. This evidence suggests that suppressing microglial activation is emerging as a promising strategy for epilepsy treatment. In the present study, our results showed a distinct spatial pattern of TRPV5 expression, with upregulation primarily in activated microglia, in the hippocampus after SE induction and LPS treatment. Additionally, I found that TRPV5 blockage by Econazole treatment attenuated microglial activation following epileptic seizures. These findings indicate that TRPV5 is involved in microglial activation under pathological conditions following epileptic insult.

Given our finding that TRPV5 inhibition suppresses microglial activation, I wondered how TRPV5 contributes to microglial-derived inflammatory events. Microglia is the key cell in brain inflammation, and microglial activation is closely related to indicating neuroinflammation^{40,41}. Moreover, microglial activation promotes a various intracellular signaling pathway, which is known to coordinate inflammatory process⁴². For instance, AKT signaling is involved in proinflammatory reaction in LPS-stimulated BV2 microglia cells⁴³ and the phosphorylated AKT acts as an upstream regulatory protein to NF-κB⁴⁴. NF-κB, a critical regulator of the inflammatory response, acts as a central mediator of the priming signal in NLRP3 inflammasome activation and induces the transcriptional expression of NLRP3⁴⁵. The NLRP3 inflammasome, a multi-protein complex comprising NLRP3 receptor, the adaptor protein ASC, and the enzyme Caspase-1, is pivotal role for the innate immune response. Activation of this inflammasome results in the cleavage of pro-Caspase-1 into its active form, Caspase-1, which in turn processes proinflammatory cytokines such as IL-1β and IL-18 into their mature, active forms, promoting cytokine release and driving further inflammation⁴⁶. In the present study, inhibition of TRPV5 led to the suppression of activated microglia, reduced the phosphorylation of AKT and NF-κB, and subsequently inhibited the formation of the NLRP3 inflammasome complex in primary microglia, thereby reducing the production of proinflammatory cytokine IL-18. These findings suggest that TRPV5 is involved in NLRP3 inflammasome formation through the AKT/NF-κB signaling pathway during microglial

activation.

Accumulating evidence suggests that seizures can trigger inflammatory responses, including further activation of microglia, creating a feedback loop that may intensify neuronal damage and worsen the disease. This dynamic suggests that inflammation in epilepsy not only results from seizures but may also contribute to their onset and progression ⁴⁷. Specifically, the release of pro-inflammatory mediators like IL-1 β and IL-18 from activated microglia enhances neuronal excitability and lowers the seizure threshold. IL-1 β , for example, promotes NMDA receptor activity by increasing tyrosine phosphorylation of NR2A/B subunits, which leads to heightened neuronal excitability ⁴². These findings underscore the importance of mitigating brain inflammation in epileptic conditions as a potential strategy to reduce seizure activity.

The present study highlights the role of TRPV5 in microglia activation following epileptic brain injury. While our results demonstrate that TRPV5 modulates inflammatory responses and microglial activation following epileptic seizures, there remains the possibility that TRPV5 could interact other cellular/molecular mechanism underlying pathogenic manifestations in neurological disorders including epilepsy. Previous study has reported that TRPV5 is upregulated in a rat osteoarthritis model, and this upregulated TRPV5 exerts the induction of chondrocyte apoptosis via the mitogen-activated protein kinase cascade and AKT/mechanistic target of rapamycin pathway in osteoarthritis ⁴⁸. Together with the present study, this evidence leads us to hypothesize that TRPV5 may be a potential regulator of several cellular/molecular mechanisms underlying pathologic development of neurological disorders, including epilepsy. Thus, exploring the functional spectrum of TRPV5 under neuropathological conditions in various neurological diseases would be interesting.



5. Conclusion

In summary, the present study demonstrates a novel evidence that microglial TRPV5 is upregulated following epileptic seizures and TRPV5 inhibition using Econazole significantly reduced microglial activation and neuroinflammatory responses, indicating that TRPV5 might be a novel regulator in microgliosis and microglial-derived neuroinflammation following epileptic seizures. Therefore, these findings suggest that targeting TRPV5 to modulate microglial activation and reduce inflammation may have therapeutic potential for epilepsy treatment.

References

1. Fisher RS, Acevedo C, Arzimanoglou A, Bogacz A, Cross JH, Elger CE, et al. ILAE official report: a practical clinical definition of epilepsy. *Epilepsia* 2014;55:475-82.
2. Sánchez J, Centanaro M, Solís J, Delgado F, Yépez L. Factors predicting the outcome following medical treatment of mesial temporal epilepsy with hippocampal sclerosis. *Seizure* 2014;23:448-53.
3. Reddy DS, Kuruba R. Experimental models of status epilepticus and neuronal injury for evaluation of therapeutic interventions. *Int J Mol Sci* 2013;14:18284-318.
4. Covolan L, Mello LE. Temporal profile of neuronal injury following pilocarpine or kainic acid-induced status epilepticus. *Epilepsy Res* 2000;39:133-52.
5. Curia G, Longo D, Biagini G, Jones RS, Avoli M. The pilocarpine model of temporal lobe epilepsy. *J Neurosci Methods* 2008;172:143-57.
6. Trinka E, Cock H, Hesdorffer D, Rossetti AO, Scheffer IE, Shinnar S, et al. A definition and classification of status epilepticus--Report of the ILAE Task Force on Classification of Status Epilepticus. *Epilepsia* 2015;56:1515-23.
7. Dalby NO, Mody I. The process of epileptogenesis: a pathophysiological approach. *Curr Opin Neurol* 2001;14:187-92.
8. McNamara JO, Huang YZ, Leonard AS. Molecular signaling mechanisms underlying epileptogenesis. *Sci STKE* 2006;2006:re12.
9. Yu C, Deng XJ, Xu D. Microglia in epilepsy. *Neurobiol Dis* 2023;185:106249.
10. Sano F, Shigetomi E, Shinozaki Y, Tsuzukiyama H, Saito K, Mikoshiba K, et al. Reactive astrocyte-driven epileptogenesis is induced by microglia initially activated following status epilepticus. *JCI Insight* 2021;6.
11. Vezzani A, Viviani B. Neuromodulatory properties of inflammatory cytokines and their impact on neuronal excitability. *Neuropharmacology* 2015;96:70-82.
12. Lee K, Jo YY, Chung G, Jung JH, Kim YH, Park CK. Functional Importance of Transient Receptor Potential (TRP) Channels in Neurological Disorders. *Front Cell Dev Biol* 2021;9:611773.
13. Kong W, Wang X, Yang X, Huang W, Han S, Yin J, et al. Activation of TRPV1 Contributes to Recurrent Febrile Seizures via Inhibiting the Microglial M2 Phenotype in the Immature Brain. *Front Cell Neurosci* 2019;13:442.

14. Wang Z, Zhou L, An D, Xu W, Wu C, Sha S, et al. TRPV4-induced inflammatory response is involved in neuronal death in pilocarpine model of temporal lobe epilepsy in mice. *Cell Death Dis* 2019;10:386.
15. Hou J, Renigunta V, Nie M, Sunq A, Himmerkus N, Quintanova C, et al. Phosphorylated claudin-16 interacts with Trpv5 and regulates transcellular calcium transport in the kidney. *Proc Natl Acad Sci U S A* 2019;116:19176-86.
16. Zhong G, Long H, Chen F, Yu Y. Oxoglaucine mediates Ca(2+) influx and activates autophagy to alleviate osteoarthritis through the TRPV5/calmodulin/CAMK-II pathway. *Br J Pharmacol* 2021;178:2931-47.
17. Wei Y, Wang Y, Wang Y, Bai L. Transient Receptor Potential Vanilloid 5 Mediates Ca2+ Influx and Inhibits Chondrocyte Autophagy in a Rat Osteoarthritis Model. *Cell Physiol Biochem* 2017;42:319-32.
18. Kumar S, Singh U, Goswami C, Singru PS. Transient receptor potential vanilloid 5 (TRPV5), a highly Ca(2+) -selective TRP channel in the rat brain: relevance to neuroendocrine regulation. *J Neuroendocrinol* 2017;29.
19. Jung H, Lee D, You H, Lee M, Kim H, Cheong E, et al. LPS induces microglial activation and GABAergic synaptic deficits in the hippocampus accompanied by prolonged cognitive impairment. *Sci Rep* 2023;13:6547.
20. Park S, Zhu J, Jeong KH, Kim WJ. Adjudin prevents neuronal damage and neuroinflammation via inhibiting mTOR activation against pilocarpine-induced status epilepticus. *Brain Res Bull* 2022;182:80-9.
21. Marrone MC, Morabito A, Giustizieri M, Chiurchiù V, Leuti A, Mattioli M, et al. TRPV1 channels are critical brain inflammation detectors and neuropathic pain biomarkers in mice. *Nat Commun* 2017;8:15292.
22. Woolf Z, Stevenson TJ, Lee K, Jung Y, Park TIH, Curtis MA, et al. Isolation of adult mouse microglia using their in vitro adherent properties. *STAR Protoc* 2021;2:100518.
23. Hughes TET, Lodowski DT, Huynh KW, Yazici A, Del Rosario J, Kapoor A, et al. Structural basis of TRPV5 channel inhibition by econazole revealed by cryo-EM. *Nat Struct Mol Biol* 2018;25:53-60.
24. He Y, Taylor N, Yao X, Bhattacharya A. Mouse primary microglia respond differently to LPS and poly(I:C) in vitro. *Sci Rep* 2021;11:10447.
25. Yaqubi M, Groh AMR, Dorion MF, Afanasiev E, Luo JXX, Hashemi H, et al. Analysis of the microglia transcriptome across the human lifespan using single cell RNA sequencing. *J Neuroinflammation* 2023;20:132.

26. Zhu J, Park S, Kim SH, Kim CH, Jeong KH, Kim WJ. Sirtuin 3 regulates astrocyte activation by reducing Notch1 signaling after status epilepticus. *Glia* 2024;72:1136-49.
27. Racine RJ. Modification of seizure activity by electrical stimulation. II. Motor seizure. *Electroencephalogr Clin Neurophysiol* 1972;32:281-94.
28. Jeong KH, Zhu J, Park S, Kim WJ. Transient Receptor Potential Vanilloid 6 Modulates Aberrant Axonal Sprouting in a Mouse Model of Pilocarpine-Induced Epilepsy. *Mol Neurobiol* 2024;61:2839-53.
29. Li X, Lin J, Hua Y, Gong J, Ding S, Du Y, et al. Agmatine Alleviates Epileptic Seizures and Hippocampal Neuronal Damage by Inhibiting Gasdermin D-Mediated Pyroptosis. *Front Pharmacol* 2021;12:627557.
30. Skrzypczak-Wiercioch A, Sałat K. Lipopolysaccharide-Induced Model of Neuroinflammation: Mechanisms of Action, Research Application and Future Directions for Its Use. *Molecules* 2022;27.
31. Cai L, Gong Q, Qi L, Xu T, Suo Q, Li X, et al. ACT001 attenuates microglia-mediated neuroinflammation after traumatic brain injury via inhibiting AKT/NFkappaB/NLRP3 pathway. *Cell Commun Signal* 2022;20:56.
32. Park S, Cho S, Kim KM, Chu MK, Kim CH, Jeong KH, et al. Honokiol-induced SIRT3 upregulation protects hippocampal neurons by suppressing inflammatory processes in pilocarpine-induced status epilepticus. *Neurochem Int* 2024;180:105873.
33. Zhang X, Liang P, Zhang Y, Wu Y, Song Y, Wang X, et al. Blockade of Kv1.3 Potassium Channel Inhibits Microglia-Mediated Neuroinflammation in Epilepsy. *Int J Mol Sci* 2022;23.
34. Nimmerjahn A, Kirchhoff F, Helmchen F. Resting microglial cells are highly dynamic surveillants of brain parenchyma in vivo. *Science* 2005;308:1314-8.
35. Vezzani A, Aronica E, Mazarati A, Pittman QJ. Epilepsy and brain inflammation. *Exp Neurol* 2013;244:11-21.
36. Möller T, Bard F, Bhattacharya A, Biber K, Campbell B, Dale E, et al. Critical data-based re-evaluation of minocycline as a putative specific microglia inhibitor. *Glia* 2016;64:1788-94.
37. Tikka T, Fiebich BL, Goldsteins G, Keinanen R, Koistinaho J. Minocycline, a tetracycline derivative, is neuroprotective against excitotoxicity by inhibiting activation and proliferation of microglia. *J Neurosci* 2001;21:2580-8.
38. Abraham J, Fox PD, Condello C, Bartolini A, Koh S. Minocycline attenuates microglia activation and blocks the long-term epileptogenic effects of early-life seizures. *Neurobiol*

Dis 2012;46:425-30.

39. Wang N, Mi X, Gao B, Gu J, Wang W, Zhang Y, et al. Minocycline inhibits brain inflammation and attenuates spontaneous recurrent seizures following pilocarpine-induced status epilepticus. *Neuroscience* 2015;287:144-56.
40. Li W, Wu J, Zeng Y, Zheng W. Neuroinflammation in epileptogenesis: from pathophysiology to therapeutic strategies. *Front Immunol* 2023;14:1269241.
41. Rana A, Musto AE. The role of inflammation in the development of epilepsy. *J Neuroinflammation* 2018;15:144.
42. Shabab T, Khanabdali R, Moghadamzusi SZ, Kadir HA, Mohan G. Neuroinflammation pathways: a general review. *Int J Neurosci* 2017;127:624-33.
43. Cianciulli A, Calvello R, Porro C, Trotta T, Salvatore R, Panaro MA. PI3k/Akt signalling pathway plays a crucial role in the anti-inflammatory effects of curcumin in LPS-activated microglia. *Int Immunopharmacol* 2016;36:282-90.
44. Ozes ON, Mayo LD, Gustin JA, Pfeffer SR, Pfeffer LM, Donner DB. NF- κ B activation by tumour necrosis factor requires the Akt serine-threonine kinase. *Nature* 1999;401:82-5.
45. Guo Q, Jin Y, Chen X, Ye X, Shen X, Lin M, et al. NF- κ B in biology and targeted therapy: new insights and translational implications. *Signal Transduct Target Ther* 2024;9:53.
46. Guo H, Callaway JB, Ting JP. Inflammasomes: mechanism of action, role in disease, and therapeutics. *Nat Med* 2015;21:677-87.
47. Vezzani A, French J, Bartfai T, Baram TZ. The role of inflammation in epilepsy. *Nat Rev Neurol* 2011;7:31-40.
48. Wei Y, Jin Z, Zhang H, Piao S, Lu J, Bai L. The Transient Receptor Potential Channel, Vanilloid 5, Induces Chondrocyte Apoptosis via Ca²⁺ CaMKII-Dependent MAPK and Akt/ mTOR Pathways in a Rat Osteoarthritis Model. *Cell Physiol Biochem* 2018;51:2309-23.

Abstract in Korean

뇌전증지속상태에 의해 유도된 미세아교세포 활성화 매개 신경염증에 대한 TRPV5의 역할

선택적 칼슘 이온 채널인 Transient Receptor Potential Vanilloid 5(TRPV5)의 발현이 최근에 대뇌의 다양한 영역에서 발현이 확인되었으나, 뇌전증성 뇌손상에 대한 TRPV5의 상세한 역할이나 기반 작용기전은 아직까지 밝혀지지 않은 상태이다. 본 연구는 필로카르핀으로 유도된 뇌전증지속상태 (Status epilepticus) 마우스 모델을 이용하여 대뇌 해마 내 TRPV5의 발현 변화를 확인하고, 일차 미세아교세포 배양을 이용하여 TRPV5 억제에 의한 미세아교세포 활성화 및 신경염증 반응의 영향을 조사하였다. 본 연구의 결과로, 필로카르핀 처리에 의한 뇌전증지속상태 유도 후 해마 내 미세아교세포에서 TRPV5 발현이 유의미하게 증가함을 처음으로 확인하였다. 배양한 해마 미세아교세포에서 Econazole에 의한 TRPV5 억제가 LPS로 유도된 미세아교세포 활성화를 감소시키고, AKT/NF-κB 신호 전달 경로 억제를 통한 NLRP3 인플라마좀 형성을 제어하였다. 또한, 필로카르핀으로 유도된 뇌전증지속상태 마우스 모델에서 TRPV5 억제는 뇌전증 발작 유도에 따른 미세아교세포 활성화의 감소를 유도하였다. 추가적으로, TRPV5 억제가 경련성 발작 및 뇌전증지속상태 발생 시간을 지연시켰다. 이러한 결과들은 TRPV5가 뇌전증 발작에 의한 미세아교세포 활성화와 이와 관련된 신경염증에 관여한다는 사실을 입증한다. 이 연구를 통해 TRPV5 억제에 의한 항염증 효과가 뇌전증성 대뇌 손상을 완화하기 위한 새로운 치료 접근법을 제공할 수 있을 것으로 기대된다.

핵심되는 말 : 뇌전증, 뇌전증지속상태, TRPV5, 미세아교세포, 신경염증